Determination of Slip Ratios in Air-Water Two-Phase Critical Flow at High Quality Levels Utilizing Holographic Techniques

Holographic techniques employing a pulse ruby laser were used to measure the size and velocity of drops for air-water two-phase critical flow at quality levels above 0.95. The use of a large numerical aperture in the holographic recording system permitted diffraction limited resolution of the droplets. The measured slip ratio along with the observation that a very significant portion of the liquid phase was concentrated near the boundary layer at the exit plane indicates that a separated flow model describing two-phase critical flow would represent the actual conditions to a better degree than the other models.

YOUNG J. LEE
MICHAEL E. FOURNEY
and
RALPH W. MOULTON

Department of Chemical Engineering
University of Washington
Seattle, Washington 98195

SCOPE

Rapid developments in the field of nuclear reactor technology in recent years have strongly stimulated the study of two-phase critical flow. A knowledge of the two-phase critical flow rate is essential for the prediction of effluent rates from an accidental break in a nuclear reactor.

Critical mass velocity of a fluid is defined as the maximum mass velocity obtainable with the fluid in a given thermodynamic state. For the critical mass velocity of a single phase fluid, the theory has been well established. However, it has been shown that the critical flow rate of gas-liquid systems is much higher than that predicted by the homogeneous equilibrium model. This model assumes that the linear velocity of each of the phase is identical, phase equilibrium exists and the specific volumes of vapor and liquid are additive. To commonly cited reasons for this are a departure from thermodynamic equilibrium, non-equilibrium (metastability) and also a difference in the linear velocity of each of phase (slip phenomena). Attempts have been made to determine the departure from equilibrium by measuring temperatures for each phase and the pressure of the mixture. In addition, slip phenomena have been studied extensively using various techniques, and yet most of the existing literature leaves much to be desired.

Other than the simple homogeneous equilibrium model several theoretical models have been proposed to predict the two-phase critical flow rate. These models have assumed that deviation from ideality is caused by either metastability or slip phenomena alone. Accounting only for slip phenomena leads to the separated flow models and accounting only for metastability leads to the homogeneous models. The absence of reliable data on slip phenomena and metastability has prevented an accurate theoretical description of two-phase critical flow phenomena. However, critical flow rates can be predicted with a fair degree of accuracy in certain quality regions with most of the models.

The most direct way of determining the slip ratio (ratio of gas velocity to liquid velocity) is by the measurement of drop size and drop velocity. Sampling and probing techniques have been suggested, but they have the undesirable characteristics of disturbing the flow. Most investigators have concluded that the distribution of drop sizes and drop velocities can be best obtained by using photographic techniques. However, the difficulty of obtaining these distributions by photographic techniques increases greatly for small size drops at high velocities. High magnification results in small areas of observation and a narrow depth of field.

The development of holographic techniques together with the use of the laser has given new hope in this field of study. Holographic techniques can record a large depth of field and three-directional movement. The laser can provide a strong and coherent light source to enable the taking of holograms for fast moving drops. Thompson et al. (1966) initiated the study of holographic techniques to measure the size distribution of droplets and Matkin (1968) extended this work to consider both the size and velocity of droplets in steam-water critical flow systems without much success due to light scattering from condensation nuclei.

The goal of this research was to measure drop size and drop velocities in air-water two-phase critical flow with an improved holographic technique. By analyzing these data and observing other details of flow phenomena closely, it was expected that one could arrive at a better understanding of two-phase critical flow systems.

CONCLUSIONS AND SIGNIFICANCE

The size and velocity of drops in air-water two-phase critical flow as well as for subcritical flows at quality levels above 0.95 has been successfully determined. This was accomplished throughout a sample volume without disturbing the flow by the use of holographic techniques with a pulsed ruby laser. Holographic techniques to record the small drops were substantially improved by using a

Correspondence concerning this paper should be addressed to R. W. Moulton. M. E. Fourney is with the Mechanics and Structure Department, University of California, Los Angeles, California 90024.

large aperture and the ruby laser was able to provide two giant pulses separated by a minimum of 5 μs.

The size distribution indicates that the number of drops increases as the size decreases. Also, these distributions show that the high velocity flow has a fewer number of larger drops than that at lower velocity for the same quality.

The results of the velocity measurements demonstrated that the range of the velocity measurements was exceedingly great even for the same range of drop size. The calculation of the average velocity for the same range of drop size indicates that the average velocity increases as the size of drops decreases and the average velocity of the drops generally increases as the gas phase velocity increases.

Slip ratios which are determined from the size distribution of drops and the average velocity of drops lie between the values calculated by two typical theories for the separated flow model (Fauske, 1962; Cruver, 1963)

$$\left\{ k = \left(\frac{V_g}{V_l} \right)^{1/2} \quad \text{and} \quad k = \left(\frac{V_g}{V_l} \right)^{1/3} \right\}$$

Furthermore, a liquid film was observed at the boundary layer of the exit plane and most of the drops were also located near the boundary layer. The above two observations in this study could be considered as a reasonable justification for using the separate flow model to represent two-phase critical flow phenomena at high qualities (qualities higher than 0.15).

Triple exposed holograms were produced by a triple pulse from the ruby laser, and these holograms showed that these techniques could be used to measure acceleration of drops.

PREVIOUS WORK

Since most nuclear reactors have used water as a coolant, a study of steam-water two-phase critical flow has been important to this development. The work of Isbin et al. (1957) is one of the earlier studies undertaken to measure the critical flow rate of steam-water mixtures through a constant area duct. Their data were found not to be complete due to the extrapolation techniques for pressure at the exit-plane. Faletti and Moulton (1963) reported the measurements of steam-water critical flow rates using a pressure tap on a concentric rod, thus permitting a detailed study of the pressure profile at both the up-stream and down-stream portions of the exit plane. They compared their data with the predictions from the simple homogeneous equilibrium model, which is an extension of the theory of single phase critical flow and found that the measured critical flow rates are much higher than that calculated from the model. Metastability and slip phenomena were suggested as possible causes for these departures.

Fauske (1962) not only confirmed the measurements of critical flow rate by Faletti and Moulton (1963) but also derived a separated flow model with the postulate that the liquid and vapor phase are separated and are in thermodynamic equilibrium so that the departure from the equilibrium behavior is attributed solely to slip. He assumed that critical flow involved maximization of the momentum average specific volume with respect to slip ratio as given by the momentum equation and found the expression for slip ratio to be

$$k = \left(\frac{V_g}{V_l} \right)^{1/2} \tag{1}$$

at critical flow.

Cruver (1963) and Moody (1963) independently assumed that critical flow involved minimization of energy requirements and differentiated the energy equation with respect to the slip ratio to obtain

$$k = \left(\frac{V_g}{V_l} \right)^{1/3} \tag{2}$$

They also proposed separated flow models based on either the momentum energy balance or the stagnation energy balance.

Levy (1965) also proposed a separated flow model based upon the momentum exchange between phases assuming that all frictional losses and head losses were negligible. The advantage of his model is that it can predict the slip ratio without any assumption. Apart from those mentioned above, a few different separated flow models (Klingebiel and Moulton, 1971; Katto, 1969) have been reported. All of these models predict the critical flow rate fairly well in the quality range from 0.01 to 1.0. However, no one verified experimentally the values for slip ratio used in these models.

Klingebiel and Moulton (1971) have reported the measurements of the slip ratio in steam-water critical flow for the quality range from 0.02 to 1.0 utilizing the impulse cage. Their results show that the measured slip ratio was much smaller than that predicted by existing models, and their discrepancies were explained as the results of entrainment of the liquid in the vapor phase. Fauske (1965) measured the void fraction in air-water critical flow using gamma ray attenuation techniques at qualities up to 0.1, and converted the data into the slip ratios. His data also were much smaller than that predicted by the separated flow models.

Matkin (1968) attempted to measure the drop size distributions and the velocity of drops in order to determine slip ratios in steam-water critical flow utilizing holographic techniques with a pulse ruby laser. The presence of condensation nuclei interfered with his program of research.

Recently Henry et al. (1970) extensively studied steam-water two-phase critical flow at low qualities and found metastability is much more significant at low quality flows. They developed a homogeneous model with an approximation of the nonequilibrium process by thermodynamic equilibrium paths, and the model exhibits good agreement with the experimental data for qualities less than 0.02.

EXPERIMENTAL EQUIPMENT

Critical Flow

Air-water was chosen as working fluid in order to avoid possible condensation nuclei effects and to minimize the metastability effects. The apparatus consisted of the equipment necessary to supply water and air at suitable conditions, together with instrumentation to measure their physical properties such as flow rate, temperature and pressure, followed by appropriate mixing devices and the test section proper. Figure 1 is a schematic diagram of the equipment.

The two phases were mixed by spraying the water into the air stream followed by passing the mixture through an aluminum honeycomb to reduce phase stratification and the scale of turbulence. After accelerating through a reducing cone the two-

phase medium entered the test section. It has already been shown that this mixing configuration does not affect the outcome of two-phase steam-water critical flow generation. A detailed description of the mixing section can be found elsewhere (Klingebiel, 1965).

The test section was a stainless steel tube 0.635 cm (0.25 in.) inner diameter and 48 cm (19 in.) long. Eight pressure taps were drilled in the wall of the test section and the closest tap to the exit plane was located 0.1143 cm (0.045 in.) away. The entire test section was insulated with asbestos tape.

Holography

Figure 2 shows the schematic diagram for the recording and the reconstruction of the holograms.

A pulsed ruby laser was built to produce single or double Q-spoiled pulses separated by a minimum of 5 μs with the pulse width being 50 ns. This laser served as the light source for holographic recording. The short exposure time provided by the ruby laser alleviated the necessity for providing vibration-free equipment generally required for holography. The energy was optically pumped through two linear xenon flash lamps (E.G.G. type FX 42-C-3) which were connected in series. A half confocal system was used as the resonator configuration and a Pockel cell (Westinghouse LPC-100) combined with a Glan-Thompson prism was used as the Q-spoiling mechanism. Details of construction, operation, and characteristics of the ruby laser used in this experiment can be found elsewhere (Lee, 1973).

The ruby laser beam was directed through the area of interest by mirrors which were front surface reflecting optical flats of good quality. Concave lenses were used to enlarge the ruby laser beam. The light level for proper exposure of the film was adjusted by varying the distance from the concave lenses to the holographic plate or the number of concave lenses used. Two kinds of film, Agfa-Gevaert 8E75 and 10E75 were used as the holographic recording material.

A He-Ne laser (Spectra-Physics Model 122) was used for the reconstruction of holograms. Two front surface mirrors were used for making the beam coaxial with the object lens of the microscope. The concave lenses, which were used to enlarge the beam for recording the hologram, were also used to enlarge the beam for reconstructing the hologram.

The reconstructed real images were formed on a rotating ground glass disk and viewed through the disc with a microscope. The rotating diffuser consisted of a carefully ground (#305 emery) glass disk spinning at 6 turns/s. The diffuser served to limit the depth of field as well as to eliminate the speckle pattern since the rotation of the diffuser completely destroyed the coherence of the background light. The rotating diffuser was attached to the microscope in such a manner that the distance from the object lens of the microscope to the ground glass could be easily adjusted. The microscope used was a Bausch and Lomb Dynazoom Microscope (Model PB 425) and the magnification could be varied from 30X to 800X. A stereo-zoom stand, Model S. K., also manufactured by Bausch and Lomb was used to support the microscope. The stereo-

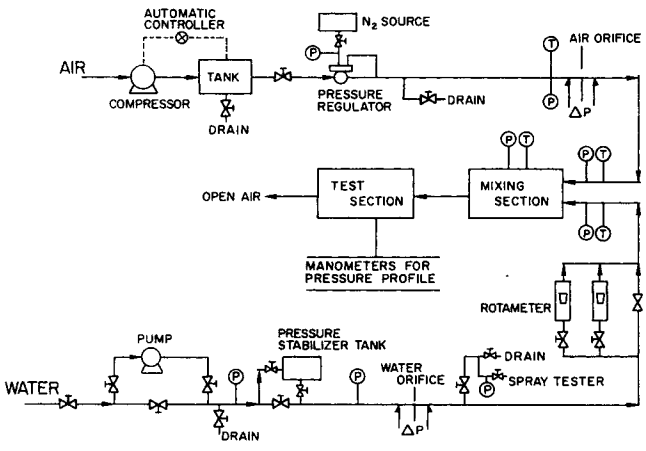

Fig. 1. Schematic diagram of critical flow equipment.

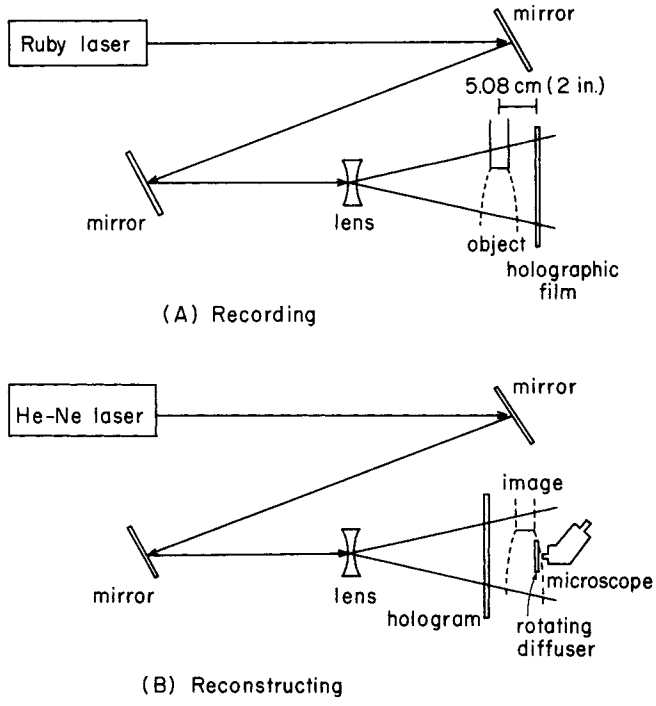

Fig. 2. Arrangement for recording and reconstructing holograms.

zoom stand enabled the microscope to move freely in three dimensions. A micrometer scale was inserted into an eyepiece of microscope in order to measure the size of the reconstructed images, and a Polaroid camera attachment was used to take photographs through the microscope.

HOLOGRAPHIC TECHNIQUES WITH A LARGE APERTURE

Matkin (1968) had some difficulties with his holographic techniques due to the limit of resolution and the large focal depth of the reconstructed image. These difficulties can be substantially improved by using a large aperture in the holographic system. This is analogous to the use of small f/number stops in ordinary microscopy.

Rayleigh criteria is one of typical expressions for the limit of resolution in ordinary optical systems.

$$\beta = 1.22\,\lambda/D \tag{3}$$

This equation states the well-known fact that for classical optics the resolution is inversely proportional to the aperture size. This is also true for holography since the holographic process can be considered as a process which merely freezes the optical wave front at a particular instant. Any process that is then performed in the wavefront to extract information will be limited by the laws of ordinary optics. Stigliani et al. (1970) have experimentally and theoretically studied these relationships including the effects of the film. These studies involved the minimum size particles that could be clearly imaged by the holographic technique. Also Bieringer and Ringlien (1971) showed an excellent reconstruction of objects of a few micron sizes using a large aperture. Their results are confirmed by the above statement.

Meier (1965) also has shown that the focal depth is limited by diffraction in holographic procedures in an identical manner to that of ordinary optics, and his relationship follows

$$\Delta z = 2f^2_{NO}\,(1/\alpha)\lambda_1 \tag{4}$$

The above equation states that the focal depth is proportional to the square of the f/number. The less the focal depth the more critical the focusing becomes. This then

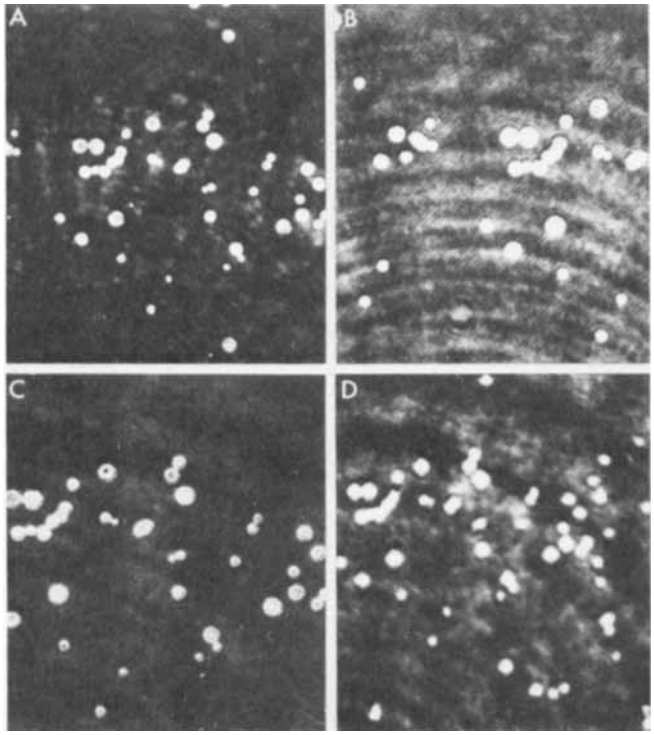

Fig. 3. Comparison among different apertures. Distance from holographic film to object: A. 5.08 cm (2 in); B. 7.62 cm (3 in); C. 10.16 cm (4 in); D. 15.24 cm (6 in).

results in less uncertainty about the drop size and its location. Locating the drops more accurately will improve the accuracy of the velocity determination.

As one goes to lower f/number optics the cost increases. However, large apertures in holography can be easily achieved by moving the holographic plate close to the volume being sampled in order to include the light from a large scattering angle.

Due to scattering properties of small drops the light intensity falls off very rapidly as the scattering angle is increased. Since the photographic film used requires light of a certain intensity there is an angle beyond which one cannot operate. This will define the f/number. This point of cutoff is a function of drop size, the film characteristics, and the method of illumination. Fortunately, the cutoff angle increases with decreasing drop diameter.

General formulas for computing the location and magnification of reconstructed images have been derived by Matkin (1968). Since a microscope was required to magnify the image, the recording and reconstruction of holograms were always made such that the conjugate real image could be observed. The location and magnification of conjugate real images are given by

$$b'_{ic} = \frac{\lambda_1 \, aa'b_i}{\lambda_2 a'(a - b_i) - \lambda_1 \, ab_i} \tag{5}$$

$$m_{ic} = \left(\frac{-a}{-a + b_i}\right)\left(\frac{-a' + b'_{ic}}{-a'}\right) \tag{6}$$

RESULTS OF HOLOGRAPHIC RECORDING

The preliminary holographic work was performed by taking holograms of 25μ glass spheres supported on a thin glass slide with the He-Ne gas laser. Figure 3 shows a comparison of the reconstructed images for different apertures. Since a complicated calculation was required to determine the exact aperture, for the sake of convenience the distance from the object to film plane was expressed as the relative aperture. Figure 3 clearly demonstrates that the resolution of the reconstructed image is improved as the aperture is increased. Considering the arrangement of the critical flow equipment and the comparison of the reconstructed images for the different apertures, it was decided to use 5.08 cm (2 in.) as the distance from object to film plane.

The average size of the glass sphere is 25μ diameter in the reconstructed images, but the smallest glass sphere shown is less than 10μ. This image has distinctive boundaries indicating that the holographic technique can record drops of only a few micron diameter.

The other purpose of using a large aperture technique was to shorten the focal depth for the reconstructed image so that the location and the velocity of the drop could be determined more accurately. The focal depth of the reconstructed image was determined from the error caused by refocusing the same image several times, and it was found that the focal depth was less than 10μ. An excellent example of the short focal depth achieved by this technique is shown in Figure 4 which consists of reconstructed images from a triple pulse exposed hologram of air-water two-phase flow. Figure 4a shows that the first two images are in focus and the third is out of focus and Figure 4b shows that the first two images are out of focus and the third is in focus. The distance between these two image planes was 20μ.

A single pulse was used to record the hologram for air-water two-phase flow from which the size of the drop could be determined. Figure 5 shows an example of the

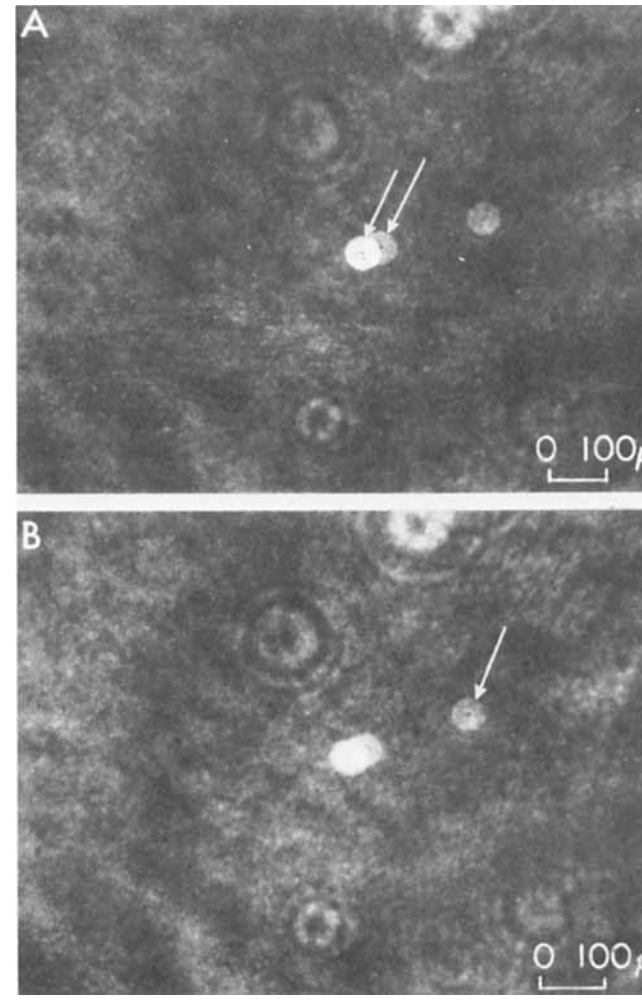

Fig. 4. Example showing depth of focal length.

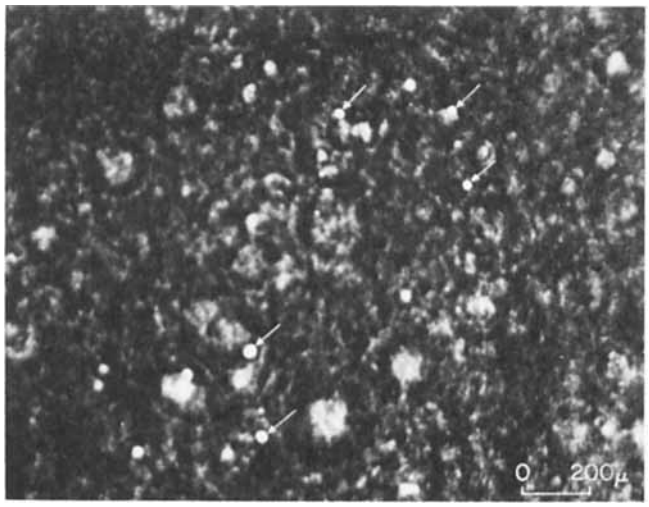

Fig. 5. Reconstructed image from single pulse exposed hologram.

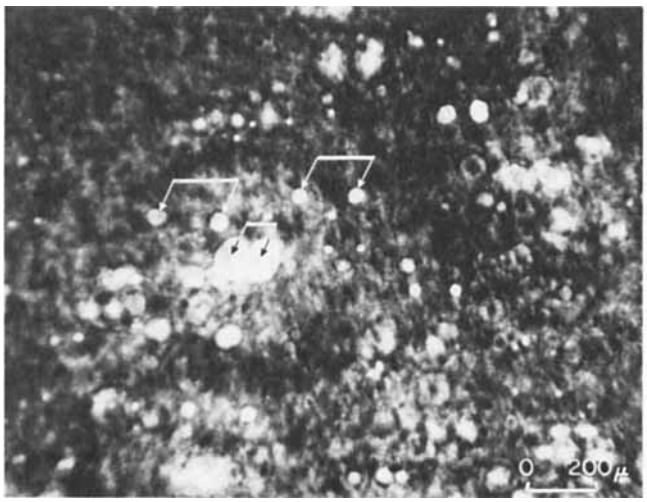

Fig. 6. Reconstructed image from double pulse exposed hologram.

reconstructed images from a single pulse exposed hologram. The quality of these reconstructed images are comparable to that of the reconstructed images from the hologram of glass spheres taken with He-Ne laser.

The reconstructed images from double giant pulse exposed holograms of air-water two-phase flow are shown in Figure 6. As mentioned previously the interval between two pulses was 5 μs. The double exposed holograms produced double images of each drop during the reconstruction. Most of the drops moved 1 to 20 times their diameter within a same image plane and there was no difficulty in tracing the movement of the drops. The intensity of both pulses should be comparable to each other in order to give comparable exposures to both images. It was found that the intensity of one pulse should be at least a quarter of the other for ease of comparison.

An unexpected triple pulse from the ruby laser produced a triple exposed hologram. Figure 7 is the reconstructed image from a triple pulse exposed hologram. These results indicate the possibility of applying triple pulse exposed holographic techniques to other areas of two-phase flow study such as the acceleration of the drop and the deformation of the drop.

The shape of the drop was mostly spherical except for some large drops. Figure 8 shows the reconstructed image of a large drop with strange shape. The image of the drop contained fringe patterns, but at this stage of the study it is not known whether these fringes are contour fringes or not and how they were formed.

There are some limitations to this technique. First, as discussed previously, the resolution of the holographic technique was limited to objects a few microns in size. Second, the holographic technique could not record the area where the drops are concentrated more than 1.5×10^4 drops/cm^3 (for a size distribution where 92% of the drops are between 10-20μ). When the drops were more highly concentrated than this, the reconstructed images became indistinguishable. This phenomenon is thought to be caused by disturbance of the reference beam and not to multiple scattering.

LABORATORY RESULTS

Two-phase Critical Flow

Accurate measurement of static pressure at the exit plane of the test section is essential for an accurate evaluation of the critical flow rate. Exit pressure was determined by extrapolation of static pressure values measured at upstream pressure taps located on the wall of the test section. An example of the pressure profile for air-water critical flow is shown in Figure 9.

Figure 10 illustrates critical flow rates measured in this research. The results are shown in the traditional manner: that is, by plotting the ratio of the experimental critical flow rate to critical flow rates calculated by the homo-

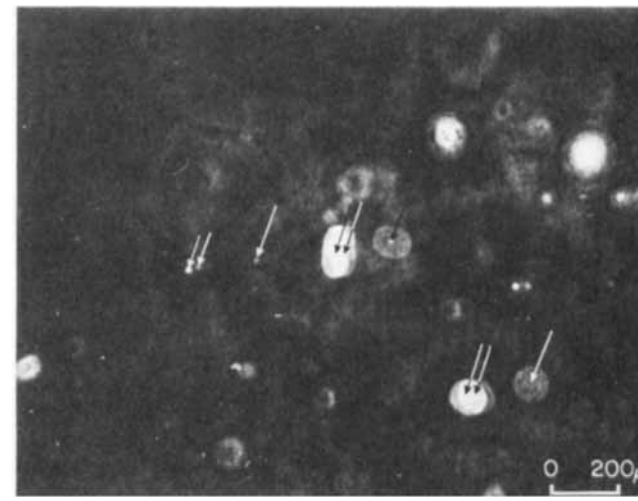

Fig. 7. Reconstructed image from triple pulse exposed hologram.

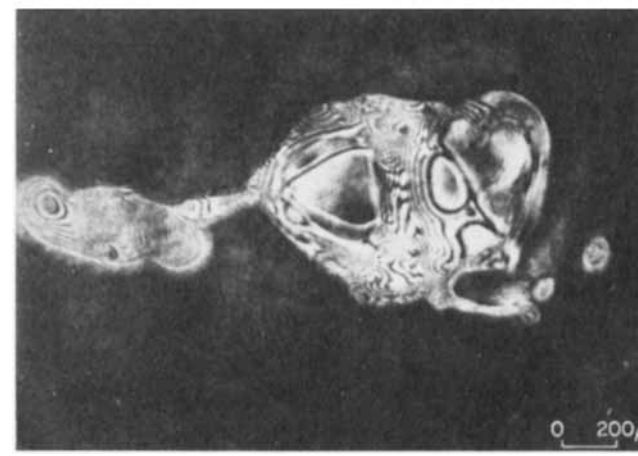

Fig. 8. Strange shape of droplet.

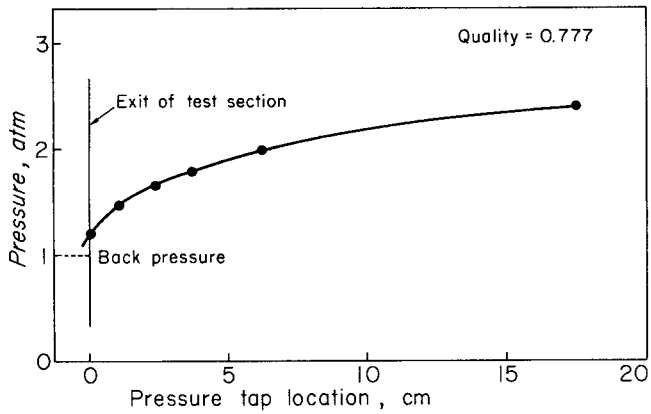

Fig. 9. Pressure profile.

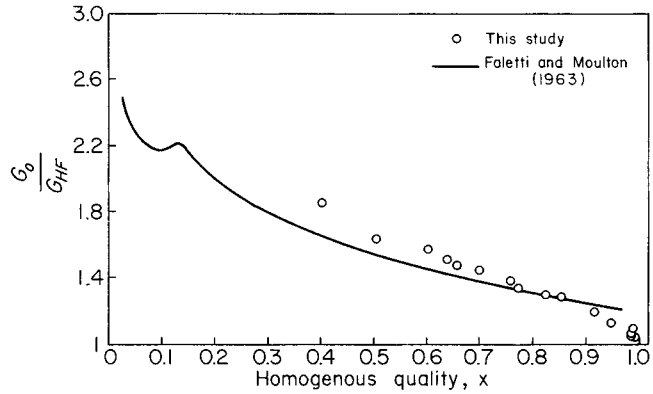

Fig. 10. Critical flow rate vs. quality.

geneous frozen model as a function of quality. The theoretical flow rate was calculated from the homogeneous frozen model instead of the homogeneous equilibrium model which has been generally used to calculate the theoretical flow rate of steam-water systems because the phase change of water in air-water critical flow is much less significant for the flow process than that in steam-water critical flow.

The analytic solution of the homogeneous frozen model was easily derived from the general expression for an expanding gas-water mixture obtained by Tangren et al. (1949)

$$G_{HF} = \sqrt{\frac{g_c P \Gamma}{x\, v_g}} \quad \text{at exit plane} \qquad (7)$$

The line in Figure 10 represents the empirical curve developed by Faletti and Moulton (1963) for steam-water critical flow for moderate pressures. At qualities lower than 0.75 the experimental points fall above the curve proposed by Faletti and Moulton (1963). These deviations might be caused by the differences in the components of two-phase flow and the theoretical model used. Also, Cruver (1963) indicated that even in steam-water systems the experimental data fall above the average curve proposed by Faletti and Moulton (1963) at low pressure. All of these comparisons indicate that this study did represent air-water two-phase critical flow.

Size Distribution

The preliminary observation of the reconstructed images might at first indicate that the drops are randomly distributed. However, generally speaking, most of the drops were located near the boundary of the jet and the average size of the drops increased with increasing distance from the center to the boundary of the jet. Therefore, it is necessary to measure the size of drops in the whole cross-sectional volume in order to obtain a reasonable size distribution. The size of the drops inside the volume of a 1-mm cylinder with a 0.25-mm distance between cylinders was measured in a wafer volume of the jet with a 1 mm thickness.

The size of individual drops could be measured to an accuracy of a micron, if necessary, but the exact size of an individual drop did not have to be known in this study. Instead it was important to determine into what range the size of the drop fell. The magnification of the microscope was fixed so that the smallest division of micrometer was 10μ. When the diameter of the drop was larger than 10μ it was not difficult to decide into what range of size the drop fell. But when the diameter of drop was near to or less than 10μ it was very difficult to decide how it should be counted. However, this error was not due to the resolution of the reconstructed image but due to other factors. This difficulty could be solved by using the higher magnification of the microscope or by taking a photograph of the reconstructed image, but both methods were too complicated to use in this work. Therefore, 10 to 20μ was chosen as the range of the smallest drops and the drops which were smaller than 10μ were included in this range.

It was found that a distribution of drop sizes could only be obtained for qualities higher than 0.95 due to limitations of the holographic technique. This was also true for velocity measurements.

Since the drops were distributed randomly, as many drops as possible were measured in order to make the measured size distribution as accurate as possible. In this respect two or three measurements at different distances from the exit plane were made for each experimental run.

Figure 11 is a typical plot of number of drops vs. size at different distances from the exit plane. These curves show the trend that the number of drops increases as the size

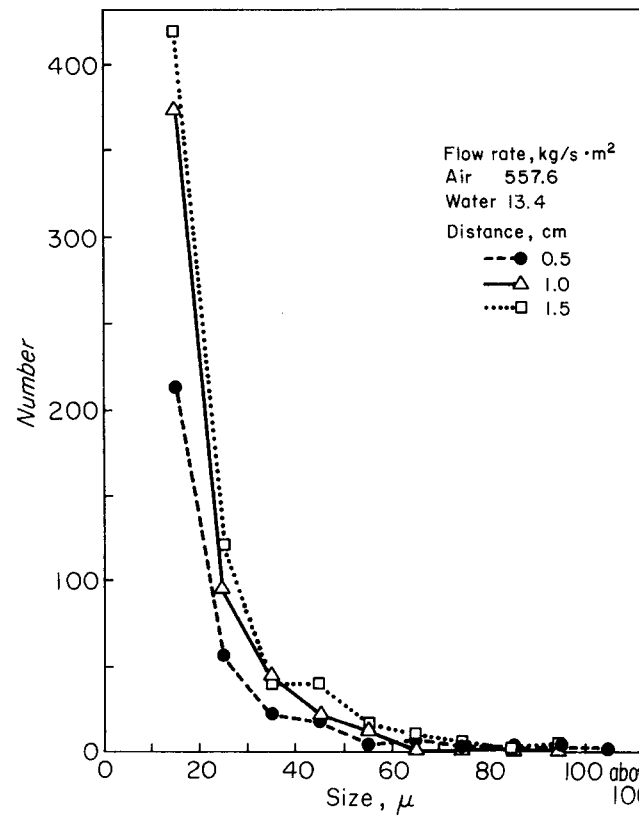

Fig. 11. Number vs. size at different distances from the exit plane.

decreases. However, when number percent of the drops was calculated as a function of size the differences among the measurements becomes less insignificant. This fact indicates that the population of drops increases with increasing distance from the exit plane, but the size distribution of the drops does not change. The increase in population of the drops with increasing distance from the exit could be explained by a decrease in the average velocity of the droplets with increasing distances from the exit plane.

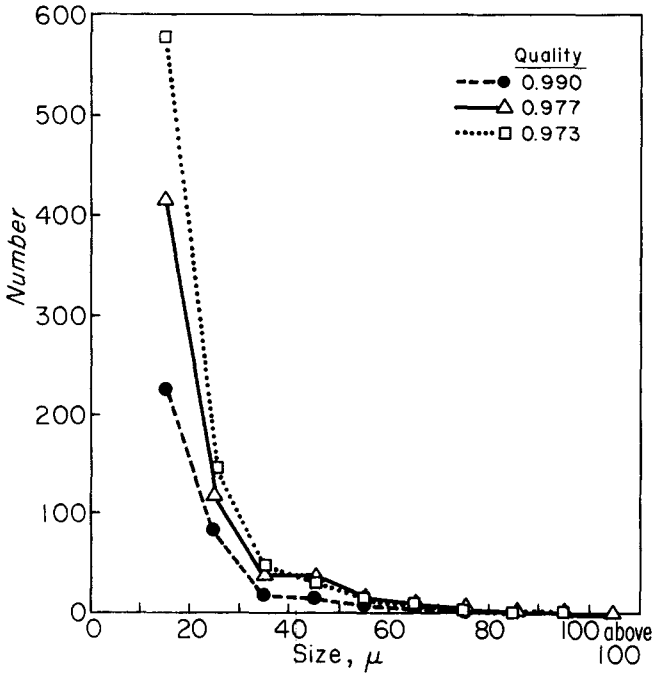

Fig. 12. Number vs. size at different qualities for critical flow (1.5 cm from the exit plane).

Figure 12 shows the number of drops vs. size for critical flow at different qualities. As expected the lower the quality of the flow the more drops are contained in the same volume. However, when the number percent and mass percent of the drop were calculated, the differences among the measurements at different qualities becomes insignificant. Similar phenomena were observed in studies at subcritical flow.

In Figure 13, mass percent vs. size are shown at different flow rates. These figures demonstrate that the high velocity flow has fewer large drops than the low velocity flow.

Literature in the study of the size distribution of drops in two-phase flow on either a theoretical or experimental basis is very limited. None of the references were concerned especially with two-phase critical flow.

Moeck and Stachiewicz (1972) have reported a theoretical study of annular-dispersed flow and have derived an equation for maximum stable drop size. Figure 14 shows a comparison between their theoretical curve and experimental data obtained in this study. The experimental values are lower than the theoretical predictions and the deviation between them increases as the air velocity increases. Since the theoretical equation was derived from experimental data obtained at moderate velocities, this deviation indicates that their theory may not be adequate to predict the maximum drop size for high velocities.

Experimental values of the mass average drop size are plotted as a function of air velocity in Figure 15. This plot could not be compared with other results since it was hard to find references on this subject. Figure 15 clearly demonstrates that the mass average drop size generally decreases with increasing air velocity. In particular the average drop size decreases sharply when the flow approaches the critical flow. These phenomena indicate the possibility that the flow characteristics, such as thickness of boundary layer or intensity of turbulence might be drastically changing when the flow rate approaches the critical value.

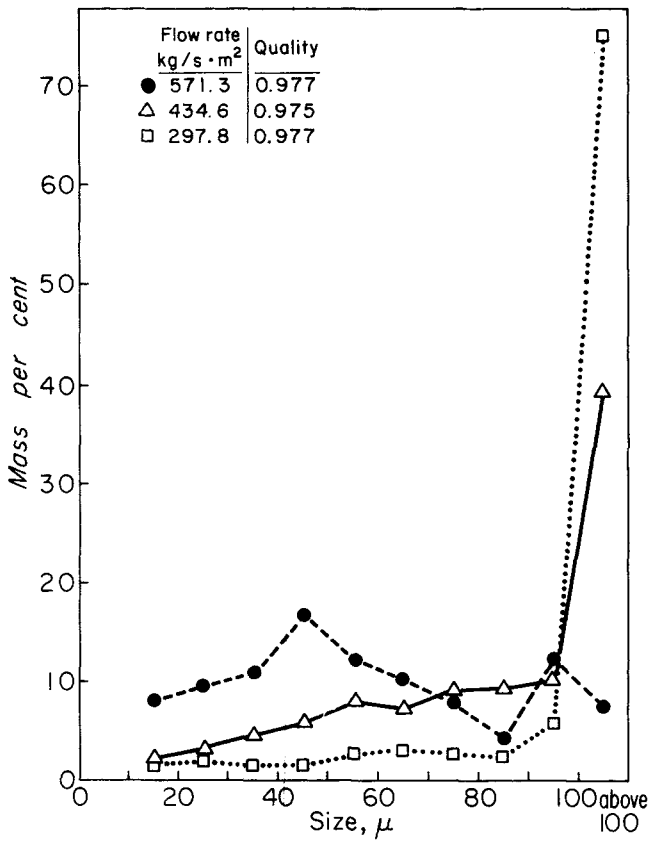

Fig. 13. Mass percent vs. size at different flow rates.

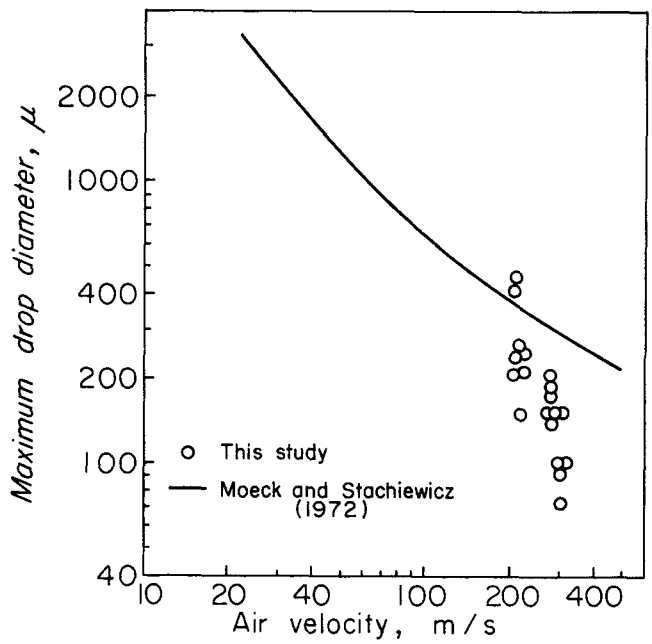

Fig. 14. Maximum drop diameter vs. air velocity.

Drop Velocity

The interval produced between the two pulses was 5 μs and most of the drops moved 1 to 20 times their diameter during this time interval. The high magnification of the reconstructed image improved the accuracy of the velocity measurements, but at the same time it worsened the ability to trace the movement of the drops. Therefore, it was important to select the most appropriate magnification. In this study the magnification of the microscope was fixed so that the smallest scale of disk corresponded to 20μ. With this magnification, there was no difficulty to tracing the movement of the drops, and the maximum error in the velocity measurement was $\pm$0.5 m/s.

Rivulets of water were observed to be broken into a stream of drops by the expanding jet at the exit plane. Since the drops from the rivulets of water would not travel as fast as the drops originally in the air flow, the velocity of the drops were measured within the boundary of the jet. Furthermore, the measurement of velocity was limited to the area within 1.5 cm from the exit because the slip ratio at the exit plane was of primary concern.

The direction of movement of the liquid drops was principally in the direction of the axis of the test section. Radial components of velocity of the drops were not considered in this study.

Figure 16 illustrates a typical plot of number percent of drops vs. velocity for different ranges of drop size. This figure shows that the range of the velocity is exceedingly wide even for the same range of drop size. It could be caused either by velocity differences at different radial positions or by the characteristics of turbulent flow, or both. The velocity plot has a Gaussian-like distribution and the breadth of the distribution curve is wider for small drops than for large drops.

Figure 17, which is a plot of the average velocity of drops vs. size at different qualities under critical flow condition, reveals that the average velocity of the drops generally increase as the size of the drops decreases. The average velocity curves for various runs are slightly different from each other. Since the fluctuations of the average velocity do not depend on the quality, it is impossible to correlate the average velocity with the quality. The number of drops whose velocity was measured ranged from several to over one hundred depending upon the range of drop size and quality. The small drops were usually mea-

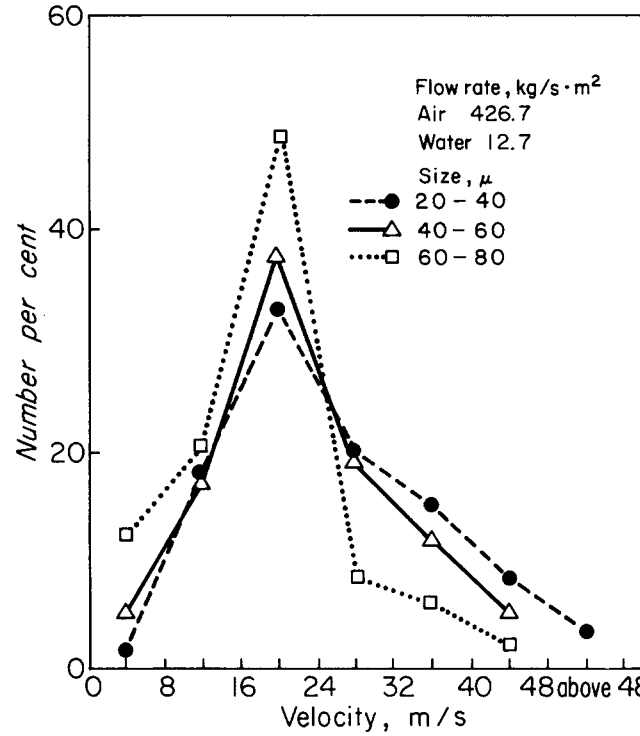

Fig. 16. Number percent vs. velocity of drop at different drop sizes.

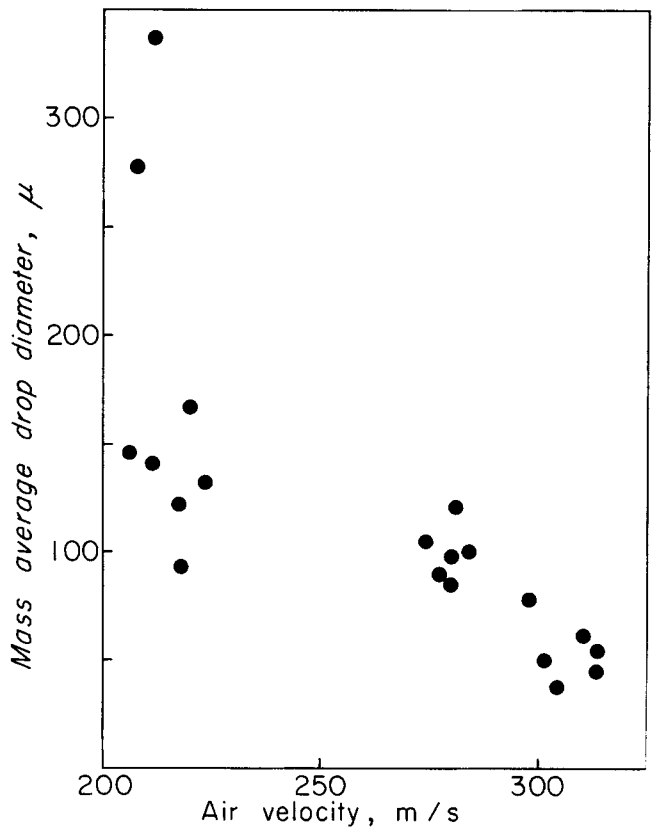

Fig. 15. Mass average drop diameter vs. air velocity.

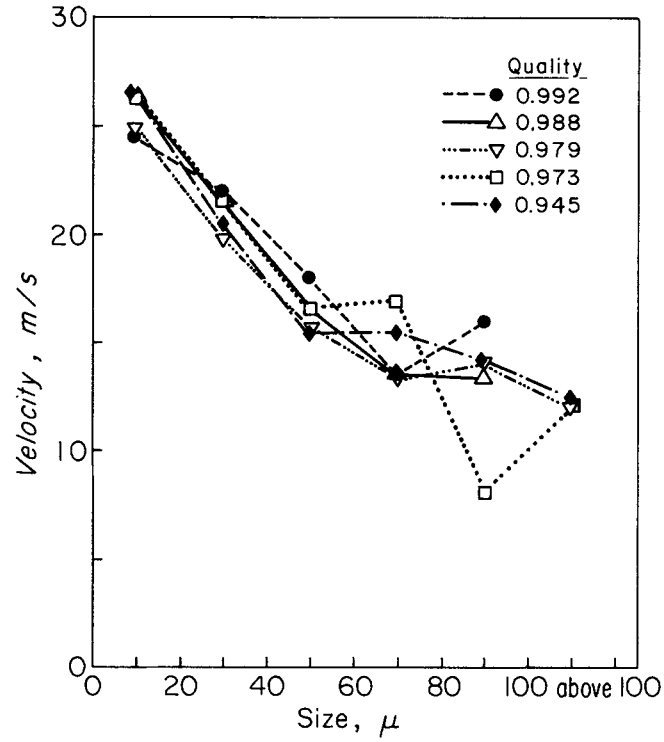

Fig. 17. Velocity vs. size at critical flow.

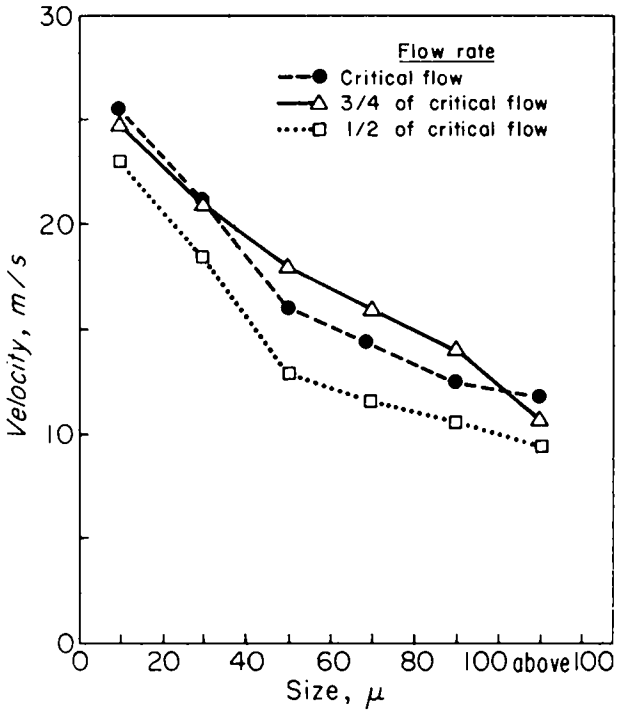

Fig. 18. Average velocity vs. drop size at different flow rates.

sured more often than the large drops. This may explain the phenomenon that the fluctuations of average velocity are generally smaller for small size drops than for large size drops.

The average velocity of the different qualities at the different flow rate is shown in Figure 18 indicating that the velocity at critical flow rate and at three-quarters of critical flow rate are similar, but the velocity at half of the critical flow rate is much lower than either of the other two. The velocities as determined in this study are affected by the absolute pressure which also varies as the flow rate is changed. Since the average gas velocity at three-quarters of the critical flow rate is slightly lower than that at the critical flow rate and the average gas velocity at a half the critical flow rate is about two-thirds of that at the critical flow rate, it can be generally said that the average velocity of the drops increases as the average gas velocity increases.

Slip Ratio

From the size distribution of drops for different conditions and the average velocity of drops shown in Figure 18, the velocity of the liquid phase was calculated from the following equation:

$$U_l = \frac{\Sigma M_{di}\, U_{di}}{\Sigma M_{di}} \qquad (8)$$

Also, the average gas velocity was calculated from the conditions at the exit plane of jet and mass flow rates measured by the orifice meter. With this information, the slip ratio was determined and is shown in Figure 19, along with experimental data reported by Klingebiel and Moulton (1971) and theoretical predictions. The relationship between slip ratio and quality at the same flow rate is not clear not only because of the fluctuations of the slip ratio but also because the range studied was too narrow. However, it is clear that the slip ratio decreases with increasing flow rate and that it becomes a minimum at critical flow condition.

DISCUSSION OF RESULTS

The slip ratios which were obtained on a theoretical basis by Fauske (1962), Levy (1965) and Cruver (1963), and by Klingebiel and Moulton (1971) from their experiments are shown in Figure 19 along with slip ratios obtained in this research.

The slip ratio values obtained by Klingebiel and Moulton (1971) are extremely low at high qualities. They reasoned that the liquid present in very high quality flow was an extremely fine mist so that almost total entrainment and consequently a slip ratio near unity would be expected. Also, Klingebiel (1965) stated that a slip ratio less than one was measured at an extremely high quality. Under these conditions extremely small liquid drops were probably present and the energy associated with a large surface area would introduce errors in the thermodynamic values associated with the liquid phase. However, his explanation completely contradicted the observations in this study that even at extremely high qualities, most of drops larger than a few microns were moving much slower than the gas phase as was also true for the liquid films existing at the boundary of jet. This fact indicates that the error in the measurements of slip ratio by Klingebiel and Moulton (1971) at high qualities was probably much larger than they realized.

The slip ratio values measured in this study are very close to the values predicted by Levy (1965) and lie between the values predicted theoretically by Fauske (1962) and by Cruver (1963). With the data of very limited qualities and conditions, it is very difficult to conclude that Levy's prediction is superior than others for predicting slip ratio in two-phase critical flow. However, it is very interesting to indicate that Levy's prediction which does not have any assumptions excepting the one of neglecting the friction loss fits the experimentally observed data in this study better than the others. Klingebiel (1965) indicated that the controversy over whether analytic expressions for slip ratio might be essentially academic

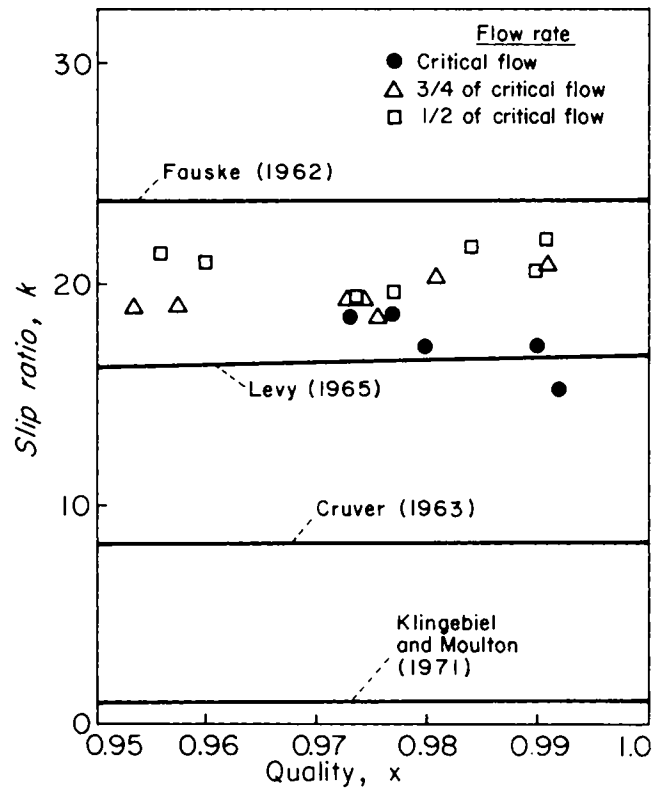

Fig. 19. Slip ratio vs. quality.

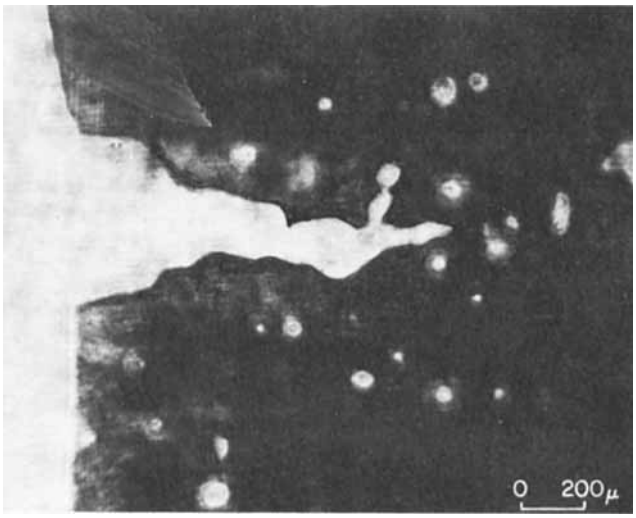

Fig. 20. Exit plane of jet.

since the effect on the critical flow rate of substituting one for the other is hardly appreciable. Therefore, it may not be of great importance whether or not the measured slip ratio in this study is close to that of a certain theory. Rather, it is important to point out that the measured slip ratios lie between the values calculated by typical theories based on the separated flow model.

Klingebiel (1965) reported that slip ratio increased with increasing flow rate at the same quality and became a maximum at the critical flow rate. He reasoned that the increasing pressure gradient near critical flow would result in an increasing difference in average velocity between vapor and liquid phases and this velocity difference would reach an upper limit only at critical flow. On the contrary, it was found in this study that the slip ratio decreased with increasing flow rate at the same quality and became a minimum at critical flow conditions. An increasing pressure gradient near the critical flow point does increase the velocity difference between the individual drops and the gas phase. Also, this increasing pressure gradient will break up the large drops into small sizes, and the average drop size becomes a minimum at critical flow as indicated previously. Slip ratio is also dependent on the average size of drops since the small drop moves faster than the larger one. Therefore, the minimum slip ratio at critical flow might be explained by the fact that the differences of average drop size affect the slip ratio more than the velocity differences near critical flow.

When the experimental data were plotted on the Baker Plot (Baker, 1954), all the data lay in the dispersed flow regimes. However, as shown in Figure 20, a liquid film was found at the boundary layer in the vicinity of the exit plane. It is important to ascertain whether the pattern observed was stable and fully developed or not. Since the ratio of the length to diameter of the test section is larger than 12, it seems quite reasonable to accept the statement that critical flow at the exit in this study is a fully developed one (Fauske, 1965). Accordingly, the existence of the liquid film demonstrates that two-phase critical flow at high quality is not entirely dispersed flow. Furthermore, it was observed that most of the drops were located near the boundary.

Theories from the separated flow model predict reasonably well the critical flow rates in spite of the simplicity of their assumption that the liquid and gas phase can be treated separately. The justification of the assumption has always been in question. Now, the credibility of the separated flow model might be strongly supported by the fact that measured slip ratio values are closer to the values calculated by typical theories of the separated flow model along with the observation that most of the drops were located near the boundary and that liquid films exist at the boundary. This observation provides a method of explaining the separated flow model, namely: two-phase flow consists principally of two separated phases; one is the gas phase at the core with negligible amounts of liquid and the other is the liquid phase at the boundary with negligible amounts of gas.

Therefore, the separated flow model is a good approximation for two-phase critical flow in the high quality region. However, in order to provide a more realistic theoretical model, the liquid film, the distribution of the drops radially as well as the extent of metastability should also be considered.

ACKNOWLEDGMENT

The financial assistance of the National Science Foundation, Grant GK-3846, is gratefully acknowledged.

NOTATION

a = distance from hologram to recording source, m
a' = distance from hologram to reconstructing source, m
b_i = distance from hologram to object plane, m
b'_{ic} = distance from hologram to conjugate image plane, m
C_l = specific heat of liquid, J/kg · K
C_p = specific heat of gas at constant pressure, J/kg · K
C_v = specific heat of gas at constant volume, J/kg · K
D = diameter of circular aperture, m
f_{NO} = f/number
G_o = observed critical flow rate kg/m² · s
G_{HF} = critical flow rate calculated from homogeneous frozen model kg/m² · s
g_c = universal gravitational constant
k = slip ratio
M = mass, kg
m_{ic} = magnification of reconstructed conjugate image
P = pressure, N/m²
U = velocity, m/s
V = specific volume, m³/kg
x = quality
Δz = focal depth, m
α = λ_2/λ_1
β = minimum angle of resolution, rad.
Γ = $\dfrac{\gamma C_p + C_l}{\gamma C_v + C_l}$
γ = M_g/M_l
λ = wave length of light, m

Subscript

di = denotes ith range of drop size
g = denotes gas phase
l = denotes liquid phase
1 = denotes recording light
2 = denotes reconstructing light

LITERATURE CITED

Baker, O., "Simultaneous Flow of Oil and Gas," *Oil Gas J.*, **53**, (12), 185 (1954).
Bieringer, R. J., and J. A. Ringlien, "Diffraction-Limited Holography," *Appl. Opt.*, **10**, 1632 (1971).
Cruver, J. E., "Metastable Critical Flow of Steam-Water Mixtures," Ph.D. thesis, Univ. of Washington, Seattle (1963).
Faletti, D. W., and R. W. Moulton, "Two-Phase Critical Flow of Steam-Water Mixtures," *AIChE J.*, 9, 247 (1963).
Fauske, H. K., "Contribution to the Theory of Two-Phase One-

Component Critical Flow," Argonne Nat. Lab., ANL-6633 (1962).
———, "Two-Phase Two- and One-Component Critical Flow," *Proc. Symp. on Two-Phase Flow*, Univ. of Exeter, England, G-101 (1965).
Henry, R. E., H. K. Fauske, and S. T. McComas, "Two-Phase Critical Flow at Low Qualities, Part I & Part II," *Nucl. Sci. Eng.*, **41**, 79 (1970).
Isbin, H. S., J. E. Moy and A. J. R. Cruz, "Two-Phase, Steam-Water Critical Flow," *AIChE J.*, **3**, 361 (1957).
Katto, Y., "Dynamics of Compressible Saturated Two-Phase Flow," *Bull. JSME*, **12**, 1417 (1969).
Klingebiel, W. J., "Critical Flow Slip Ratios of Steam-Water Mixtures," Ph.D. thesis, Univ. of Washington, Seattle (1965).
——— and R. W. Moulton, "Analysis of Flow Choking of Two-Phase, One-Component Mixtures," *AIChE J.*, **17**, 383 (1971).
Lee, Y. J., "An Application of Holography to the Study of Air-Water Two-Phase Critical Flow," Ph.D. thesis, Univ. of Washington, Seattle (1973).
Levy, S., "Prediction of Two-Phase Critical Flow Rate," *J. Heat Transfer*, **87**, 53 (1965).
Matkin, J. H., "Determination of Aerosol Size and Velocity by Holography and Steam-Water Critical Flow," Ph.D. thesis, Univ. of Washington (1968).
Meier, R. W., "Depth of Focus and Depth of Field in Holography," *J. Opt. Soc. Am.*, **55**, 1963 (1965).
Moeck, E. O., and J. W. Stachiewicz, "A Droplet Interchange Model for Annular-Dispersed, Two-Phase Flow," *Intern. J. Heat Mass Transfer*, **15**, 637 (1972).
Moody, F. J., "Maximum Flow Rate of a Single Component, Two-Phase Mixture," General Electric Rept., APED-4378 (1963).
Stigliani, D. J., Jr., R. Mittra, and R. G. Semonin, "Particle-Size Measurement Using Forward-Scattering Holography," *J. Opt. Soc. Am.*, **60**, 1059 (1970).
Tangren, R. F., C. H. Dodge, and H. S. Seifert, "Compressibility Effects in Two-Phase Flow," *J. Appl. Phys.*, **20**, 637 (1949).
Thompson, B. J., G. B. Parrent, J. H. Ward, and B. Justh, "A Readout Technique for the Laser Fog Disdrometer," *J. Appl. Meteor.*, **5**, 343 (1966).

Manuscript received July 27, 1973; revision received November 8 and accepted November 9, 1973.

Molecular Oxygen Induced Crystallite Size Effect in Reduction of Nitric Oxide with Ammonia Over Supported Platinum

The effect of changing platinum crystallite size from 2.7 to 15.5 nm on the specific catalytic activity in NO reduction by NH_3, with and without added O_2, was studied over alumina supported platinum catalysts between 423 and 473°K. In the NO-NH_3 system both specific catalytic activity and selectivity to N_2 are independent of crystallite size. In the NO-O_2-NH_3 system the specific catalytic activity of the 15.5 nm crystallites is about six times that of the 2.7 nm crystallites. The NO reduction rate shows dependence on NO to the first power and on NH_3 to the one-half power.

ROBERT J. PUSATERI
JAMES R. KATZER
and WILLIAM H. MANOGUE

Department of Chemical Engineering
University of Delaware
Newark, Delaware 19711

SCOPE

Supported noble metal catalysts find wide and important application in industry and are gaining importance in pollution control applications including the reduction of NO in automotive exhaust and in tail gas streams. Because of the high cost of noble metals, these catalysts usually contain only a small amount of highly dispersed metal on a support. The metal crystallites typically range from 1.0 to 50 nm in diameter (1 nm = 10Å). The literature provides little quantitative information on their kinetic behavior in NO reduction, and it provides no information on the effect of the degree of dispersion of the metal on its specific catalytic activity (rate of reaction per unit metal surface area) in such reactions. In many reactions involving H_2 and hydrocarbons the specific catalytic activity is independent of the size of the metal crystallites. However, it has recently been shown that in oxidation with O_2, including NH_3 oxidation, the specific catalytic activity is markedly dependent on crystallite size. The cause of this effect can be better understood if information on related oxidation-reduction reactions is available; yet there are no data with other oxidants such as NO. This work sought to determine if a crystallite size effect exists for a platinum on alumina catalyst in the reduction of NO by NH_3 with and without added O_2. Another purpose of the work was to quantitatively determine the kinetics of the NO-NH_3 reaction.

Correspondence concerning this paper should be addressed to J. R. Katzer. R. J. Pusateri is with Hercules Research Center, Hercules, Inc., Wilmington, Delaware. W. H. Manogue is with the Experimental Station, E. I. duPont de Nemours and Company, Wilmington, Delaware.